This is an author-deposited version published in: http://oatao.univ-toulouse.fr/
Eprints ID: 2524

To cite this document: Hissler, Christophe and Probst, Jean-Luc (2006) *Chlor-alkali industrial contamination and riverine transport of mercury: Distribution and partitioning of mercury between water, suspended matter, and bottom sediment of the Thur River, France.* Applied Geochemistry, 21 (11). pp. 1837-1854. ISSN 0883-2927

Any correspondence concerning this service should be sent to the repository administrator: staff-oatao@inp-toulouse.fr

Chlor-alkali industrial contamination and riverine transport of mercury: Distribution and partitioning of mercury between water, suspended matter, and bottom sediment of the Thur River, France

Christophe Hissler, Jean-Luc Probst *

Institut National Polytechnique (INP), Ecole Nationale Supérieure Agronomique de Toulouse (ENSAT), Laboratoire Agronomie Environnement Ecotoxicologie (AEE), Avenue de l'Agrobiopole, BP 32 607, Auzeville-Tolosane, 31326 Castanet-Tolosan Cedex, France

Abstract

Total dissolved and total particulate Hg mass balances were estimated during one hydrological period (July 2001–June 2002) in the Thur River basin, which is heavily polluted by chlor-alkali industrial activity. The seasonal variations of the Hg dynamics in the aquatic environment were assessed using total Hg concentrations in bottom sediment and suspended matter, and total and reactive dissolved Hg concentrations in the water. The impact of the chlor-alkali plant (CAP) remains the largest concern for Hg contamination of this river system. Upstream from the CAP, the Hg partitioning between dissolved and particulate phases was principally controlled by the dissolved fraction due to snow melting during spring high flow, while during low flow, Hg was primarily adsorbed onto particulates. Downstream from the CAP, the Hg partitioning is controlled by the concentration of dissolved organic and inorganic ligands and by the total suspended sediment (TSS) concentrations. Nevertheless, the particulate fluxes were five times higher than the dissolved ones. Most of the total annual flux of Hg supplied by the CAP to the river is transported to the outlet of the catchment (total Hg flux: 70 $\mu g \, m^{-2} \, a^{-1}$). Downstream from the CAP, the bottom sediment, mainly composed of coarse sediment (>63 μm) and depleted in organic matter, has a weak capacity to trap Hg in the river channel and the stock of Hg is low (4 $mg \, m^{-2}$) showing that the residence time of Hg in this river is short.

1. Introduction

Industrialization of the Thur valley, France, began in the 18th century and has since increased, introducing many pollutants into the environment. The principal source of Hg contamination in this area is an industrial chlor-alkali plant. Industrial installations in this area have had a negligible impact on the global Hg cycle (Nriagu and Pacyna, 1988), but locally they release a significant amount of Hg to the atmosphere and rivers, creating diffuse and point source persistent contamination of the Thur River ecosystem (Maserti and Ferrara, 1991;

---

* Corresponding author. Tel.: +33 5 62 193949; fax: +33 5 62 193901.
  E-mail addresses: christophe.hissler@ensat.fr (C. Hissler), jean-luc.probst@ensat.fr (J.-L. Probst).

Ferrara et al., 1992; Calasans and Malm, 1997; Lodenius, 1998; Sensen and Richardson, 2002; Biester et al., 2002a,b; Hissler and Probst, 2006). Incidents of Hg poisoning of Almadén miners in Spain, in the 16th century (Menendez-Navarro, 1996) and, more recently, of the people of Minamata Bay, Japan, in 1953 (Osame and Takizawa, 2001) and in Iraq in 1970 (Bakir et al., 1973), revealed the lethal potential of Hg. Thus, in 1973, the Alsatian community realized the significance of Hg pollution, resulting in a significant decrease of industrial Hg wastes in the Thur River basin. However, recent studies (Probst et al., 1999; Hissler et al., 2003, in press; Remy et al., 2003b) has shown the persistence of Hg pollution in this area. It became important to determine the fate and behavior of Hg released in the Thur River because of potential Hg contamination of surface water and also groundwater. Groundwater contamination is especially important in this region because the direction of the water exchange is from the river to groundwater (Duprat et al., 1979; Esteves, 1989).

Multiple forms of Hg may be found in aquatic environments depending on the physical and chemical characteristics of water, which control its behavior. Mercury associates with the dissolved organic matter (Schuster, 1991) or other inorganic solute compounds, such as Cl and Br (Ravichandran, 2004) and forms stable metallic aqueous complexes. This complex stability increases the dissolved fraction of Hg in the water column and consequently, the capacity of Hg transfer to groundwater (used in this region as drinking water) and aquatic organisms.

The objective of this study was to follow the fate of Hg in the Thur River, which is heavily polluted by a CAP, particularly downstream from the industrial effluents. The influence of hydrological and physicochemical conditions on the fluvial transport of Hg and the partitioning of Hg between the particulate and dissolved phases were also determined.

2. Site description

2.1. The Thur River basin

The Thur River drains about $270 \, km^2$ in the Southern Vosges Mountains located 100 km SW of Strasbourg (Fig. 1). The drainage basin extends from the high crystalline Vosges Mountains (66% of the basin area) to the Alsatian plain, where the Thur River merges with the Ill River, a tributary
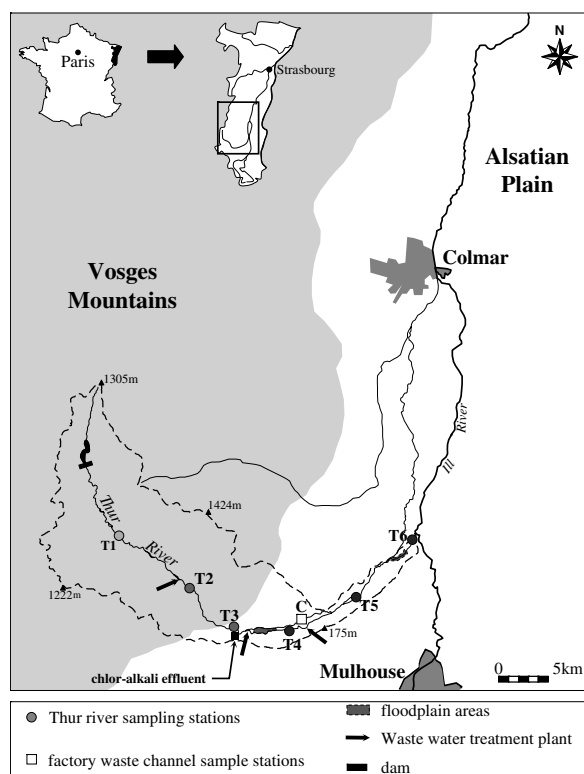

Fig. 1. Geographic location map of the Thur River basin and of the 8 sampling stations.

of the Rhine River. The Thur River contributes significantly to the groundwater supply, which is important in Alsace for the economy and hydrosystem equilibrium.

The Thur River basin is characterized by a temperate oceanic mountainous climate. Westerly winds dominate and the drainage basin receives significant precipitation throughout the year (Fig. 2).
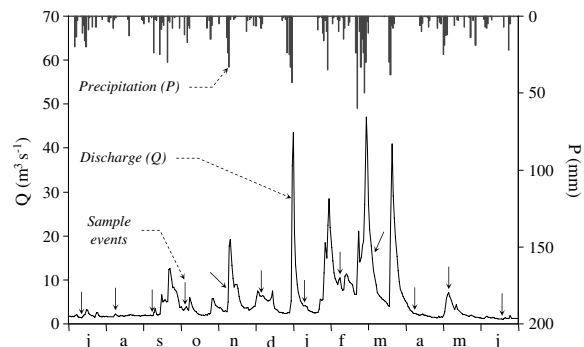

Fig. 2. Evolution of the mean daily discharge (Q in $m^3 \, s^{-1}$) and of the precipitation amount (P in mm) at the station T2 between July 2001 and July 2002. The arrows represent the periods of sampling.

The seasonal discharge regime is strongly influenced by the amount of precipitation in the mountains (1500 mm a^{-1} at T2), which is lowest in summer and highest in winter. Generally, snow represents 25% of the precipitation and covers the highest elevations (>500 m) for about 3 months/year. The major hydrological events are snowmelt and storms, which can produce important discharges of short duration (Fig. 2). The Thur River discharge undergoes strong variations during the year: a period of low water flow from May until September (mean seasonal discharge of 2.9 $m^3 s^{-1}$ at station T2) and a period of high water flow from November until March (mean seasonal discharge of 7.3 $m^3 s^{-1}$ at T2).

The economic importance of this region greatly affects the hydrodynamics of the riverbed. A dam situated in the upper part of the basin (upstream from station T1) regulates the annual discharge, but it also traps significant suspended sediment from upstream soil erosion. The most important part of the river channel, between stations T1 and T6, is embanked (about 10 m in elevation) and is characterized by intensive river bottom erosion, but negligible bank erosion. Downstream from the mountainous area, only 10% of the riverbed is flood plain (Fig. 1).

2.2. The chlor-alkali plant (CAP)

The chlor-alkali electrolysis process results in the manufacture of Cl_2, H_2 and NaOH caustic solution. The electrolytic cell consists of an electrolyzer and a decomposer. In the electrolyzer section, a NaCl brine solution flows concurrently with a Hg cathode. Cl_2 gas forms at the anode and Na forms an amalgam with Hg in the cathode. The amalgam is separated from the brine and enters in the decomposer section, where it reacts with deionized water to produce NaOH and volatile H_2 gas. Mercury released from the amalgam goes back to the electrolyzer section following a continuous flow.

In 1970, the chemical plant of the Thur River basin released 120 g of Hg/ton of Cl_2 produced, or about 8 t of Hg/a, of which 80% was released as sewage effluent into the Thur River and 8% directly into the atmosphere. Such Hg losses are similar to those estimated by Vernet and Thomas (1972) for the Canadian chemical industry (7 t of Hg released into the nearby aquatic ecosystem and 1 t into the atmosphere/a). After 1970, the total amount of Hg released in the Thur River basin was drastically reduced, and in 2000, the Hg loss decreased to under 3 g of Hg/t of Cl_2 produced, i.e., 130 kg of Hg/a, but the proportion released into the atmosphere (77%) was significantly higher (Hissler and Probst, 2006).

3. Materials and methods

3.1. Sampling and pre-analysis procedures

Water samples were collected in two periods. First, in November 2000, all the main tributaries were sampled to characterize the spatial evolution of the chemical composition of the river water. From July 2001 to June 2002, water was collected from eight sample stations to determine the longitudinal and seasonal geochemical variation of the river going from less polluted water (T1, T2 and T3), upstream from the CAP, to the more contaminated ones (T4, T5 and T6) downstream from the CAP. Two stations, CAE and C, were collected from two industrial effluent channels. Samples at CAE were collected 2 m downstream of the CAP discharge pipe and 100 m upstream from the confluence with the Thur River. The annual average discharge of this effluent channel and of the river at their confluence were 0.4 $m^3 s^{-1}$ and 5.5 $m^3 s^{-1}$, respectively. Samples at site C were collected downstream from all the industrial discharge pipes and 4 km upstream from the confluence between the channel and the Thur River. The annual average discharge of channel C and the Thur River at T4 were 2.5 and 3.0 $m^3 s^{-1}$, respectively.

The river water was collected at 20 cm depth in the middle of the main channel, in Teflon PFA bottles previously rinsed in the river. The samples were stored at 4 °C until they were filtered about 5 h later. The water samples were filtered in the laboratory using a Teflon system with Hg clean N_2 and hydrophilic PTFE Teflon filters ($\varnothing < 0.45$ μm, Millipore©), soaked in HCl (25%) for 3 days before filtration. The solution that passed through the filter consisted of dissolved ions and some colloids <0.45 μm.

Total suspended sediment (TSS) and the associated total particulate Hg collected on the filters at −20 °C were preserved until digestion. For the total dissolved Hg (Hg_T^d) analysis, the samples were first oxidized using 0.5% BrCl (0.2 N), in order to destroy organic Hg complexes. Then, they were stored in Teflon PFA flasks at 4 °C and subsequently analyzed within 2 days of filtration. The reactive dissolved Hg (Hg_R^d) was directly analyzed

in the filtrate without addition of any reagent and corresponds to the Hg, which is easily reduced to Hg^0 during the reaction with $SnCl_2$ at pH 1 (Mason et al., 1993). This fraction includes mostly ionic (Hg^{2+}) plus dissolved gaseous Hg (DGM), but also the Hg fraction weakly bound to inorganic ($Hg(OH)_2$, $HgCl_2$) and organic complexes (Coquery et al., 1997). It is characterized as the fraction of Hg that may be more easily released into the aquatic environments. Indeed, Hg associated with dissolved organic matter is strongly bound and can not be released in such conditions (Ravichandran, 2004).

The analysis of dissolved organic carbon (DOC) was made directly after filtration. Glass dishes have been washed with 10% HCl, rinsed with ultrapure water (Millipore, UHP) and burned at 600 °C in a clean oven in order to destroy all traces of organic matter. The samples used for determination of the dissolved cations and anions were stored in polyethylene flasks at 4 °C and were analyzed within 2 weeks.

River bottom sediment samples were collected in two periods. The authors first sampled every 2 months at all sites (T1–T6) between July 2001 and June 2002. A second sampling was carried out during low water flow in December 2001, between stations T3 and T6. Eighty five samples of riverbed sediment were collected (on average one sample per 250 m). Each sediment sample was a composite of 5–10 sub-samples. All the samples were stored in polyethylene bags at 4 °C, were dried in glass dishes in a clean room for 2 weeks at 20 °C, and sieved through 2 mm and 63 μm nylon screens.

Measurement of Hg was made in stream sediment (bottom and suspended) following sample digestion in 60 mL savilex with 12 mL of HNO_3: HCl: BrCl (4:1:1) at 90 °C for 14 h (Remy et al., 2003b). Clean procedures were followed to avoid Hg contamination during sampling, storage and analysis (Quesmerais and Cossa, 1997). Different sites were sampled the same day, and thus, hydrological conditions were the same for all stations.

3.2. Analytical methods

Total Hg was measured in soil and river sediment samples using Cold Vapor atomic fluorescence spectrometry (CV-AFS). This system consisted of an atomic fluorescence spectrometer (PS Analytical, Merlin Plus) coupled with a continuous vapor flow generator. Total Hg measurement was performed by reduction with $SnCl_2$ solution. The detection limit for solid material was 0.3 ng g^{-1} for a sample aliquot of 200 mg and the coefficient of variation determined on three replicate analyses was <10%. During digestion and analysis, reference material was analyzed every 13 samples and blanks every six samples. Recovery and accuracy were tested using a river bottom sediment certified reference material (CRM 320). The average value obtained ($n = 10$) was 94.2% for the recovery of total Hg and 4.1% for the accuracy of the certified value.

Total Hg and reactive dissolved Hg were measured by CV-AFS after addition of NH_2OHHCl (for total dissolved Hg samples only), then $SnCl_2$ reduction, and Au amalgamation trapping. A detection limit of 0.12 ng L^{-1} was achieved and the coefficient of variation was at most 10% as determined by three replicate analyses of all water samples.

The water pH was measured twice, during sampling and in the laboratory after filtration. The alkalinity was measured by Gran titration using a Mettler DL 40. The analysis of DOC was directly made after filtration using a SHIMATZU TOC 5000, with a precision of 0.1 mg L^{-1}. The dissolved cation (Na^+, K^+, Ca^{2+}, Mg^{2+}) and anion (Cl^-, NO_3^-, SO_4^{2-}) analyses were made using atomic absorption spectrometry (HITACHI® Z-8200) and Ion Chromatography (DIONEX®), respectively. The chemical composition of river sediment was determined using ICP-AES (Jobin Yvon® 124) for the major elements and Sc after a $LiBO_3$ fusion method, and Infrared Spectrometry (LECO® CS 125 analyzer) for Organic C (OC) content.

3.3. Flux calculations

The seasonal flux of dissolved and particulate Hg was estimated at the seven sample stations distributed along the Thur River. Calculations were made using daily discharges and monthly measurement of TSS and Hg concentration. Due to the low frequency sampling of TSS, the seasonal TSS flux was obtained using the database of the Rhin-Meuse French Water Agency (period 1971–2002) and we calculated from these data the relationship between the TSS flux (F_{TSS} in g s^{-1}) and the river discharge (Q in m^3 s^{-1}) for each available station as follows (Eq. (1)):

$$F_{TSS} = bQ^a \tag{1}$$

where the coefficients a and b are derived for each sample station from the coefficients of the linear regression calculated between $\log(F_{TSS})$ and $\log(Q)$
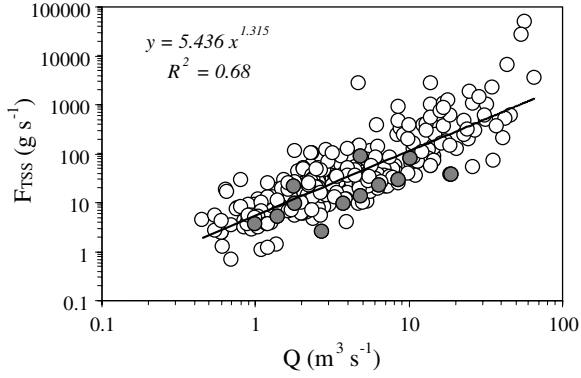
Fig. 3. Relation between the Thur River discharge and flux of total suspended sediment (F_{TSS}) at the T5 sampling station. Open circles represent the data obtained using the total suspended sediment concentration from the Water Agency database and grey circles the data obtained during this study.

e.g., the coefficients a and b are 1.315 and 5.436 for station T5, respectively (Fig. 3).

Using the mean daily discharge, the corresponding daily TSS flux was calculated using Eq. (1) for each sample station. The annual TSS flux was calculated by summing the daily fluxes. The particulate Hg fluxes were calculated for each homogeneous hydrological period (high water flow, low water flow, flood event) by multiplying the average particulate Hg concentration measured and the average TSS flux calculated during this period. The annual particulate Hg flux was obtained by summing the flux calculated for each period.

The dissolved Hg flux for each hydrological period was calculated by multiplying the average river discharge by the average dissolved Hg concentration. The annual dissolved Hg flux was then obtained by summing the flux calculated for the different periods.

3.4. Mercury stock in the river bottom sediments

The total stock of Hg in the river sediments was estimated for the main channel of the Thur River, between T3 and the outlet of the basin. This part of the river represents the alluvial plain and is directly affected by the chlor-alkali effluents. Two types of samples were distinguished. The bottom load sediment samples were taken in the middle of the channel (riverbed sediment) with a spatial resolution of one sample per 250 m. Riverbank sediments were also collected in all the areas where finest sediment accumulates. The total stock of Hg

is the sum of the Hg trapped in the bottom load and the Hg trapped in the riverbank (Eq. (2)).

$$S^{Hg} = \sum_{k=1}^{3} \left\{ \sum_{i=1}^{n} ([Hg]_i^{RS} \times M_i^{RS}) + [Hg]_k^{RL} \times M_k^{RL} \right\} \tag{2}$$

where S^{Hg} is the stock (in g) of total Hg trapped in the river bottom sediment between T3 and T6, $[Hg]_i^{RS}$ ($\mu g\ g^{-1}$) is the total Hg concentration in each riverbank area i, $[Hg]_k^{RL}$ ($\mu g\ g^{-1}$) is the average total Hg concentration in the bottom load of the different sections k of the river (T3–T4, T4–T5 and T5–T6), M_i^{RS} (kg) is the quantity of sediment in each riverbank area, and M_k^{RL} (kg) is the quantity of bottom sediment in the different sections k of the river.

The top 10 cm of sediment used for this estimation represented a time-integrated sample, which possibly introduces temporal variability into spatial data. Although the rate of sediment deposition shows some variation between each stretch of the riverbed, the top 10 cm includes recent sediment along with older material and this sample reflects the overall spatial distribution of Hg within the surficial bottom sediment (Birkett et al., 2002).

4. Results and discussion

4.1. Hydrological conditions of sampling

During the period between July 2001 and June 2002, the river discharge was quite similar at all the sample stations, depending on the amount of precipitation that fell in the whole basin (Fig. 2). The mean annual discharge ranged from $3.7\ m^3\ s^{-1}$ at T1 to $6.9\ m^3\ s^{-1}$ at T5 and $5.7\ m^3\ s^{-1}$ at the outlet of the basin (Table 1). The highest water discharge occurred between January and April, with a maximum of $47\ m^3\ s^{-1}$ at T2 and of $68\ m^3\ s^{-1}$ at T5. The lowest water discharge was found between June and September and ranged from 0.1 to $2.0\ m^3\ s^{-1}$ at the different sample stations. The study period presented a normal annual runoff ($1100\ mm\ a^{-1}$) compared with the hydroclimatic records of the last 30 a. The deviation with the mean interannual runoff (1971–2002) was less than 5%.

4.2. Total suspended sediment (TSS) variation and flux

Concentration of TSS and corresponding riverine flux is known to vary enormously over time and space

Table 1
Mean, maximum and minimum values for river water discharge (Q), pH, suspended sediment concentration (TSS), Cl^- concentration, dissolved organic C concentration (DOC), reactive (Hg_R^d), total dissolved (Hg_T^d) and particulate Hg (Hg_T^p) concentrations, and median value ($n = 6$) of Hg enrichment factor (EF_{Hg}^{Sc}) at the eight sampling stations between July 2001 and June 2002

Sample stations		Q m³ s⁻¹	pH	TSS mg L⁻¹	Cl^- mg L⁻¹	DOC mg L⁻¹	Hg_R^d ng L⁻¹	Hg_T^d ng L⁻¹	Hg_T^p µg g⁻¹	EF_{Hg}^{Sc}
T1	Mean	3.7	7.3	5.5	6.7	1.3	–	0.7	0.55	20
	Max.	27.8	7.4	30.0	8.5	2.0	–	2.4	1.9	
	Min.	1.1	7.1	0.2	4.5	1.0	–	<0.1	0.05	
T2	Mean	5.5	7.6	4.7	9.0	1.8	–	0.9	0.75	41
	Max.	47.0	7.8	22.0	12.9	2.6	–	2.3	4.9	
	Min.	1.0	7.3	1.0	6.6	1.3	–	<0.1	0.12	
T3	Mean	5.4	7.6	4.2	9.1	1.8	–	1.3	0.43	81
	Max.	45.7	7.8	14.2	13.3	3.0	–	5.5	1.5	
	Min.	1.1	7.3	1.0	6.1	1.2	–	<0.1	0.13	
T4	Mean	3.1	7.6	5.4	65.5	2.3	6.2	91	28	411
	Max.	28.8	8.0	14.0	143	3.8	16	270	190	
	Min.	0.3	7.4	1.4	16.3	1.5	1.1	17	3.6	
C	Mean	2.5	7.7	5.3	49.0	4.9	11	100	26	478
	Max.	8.0	8.3	16.2	97.5	18.2	56	540	110	
	Min.	0.2	7.2	1.7	18.4	1.4	0.9	8.2	4.8	
T5	Mean	6.9	7.7	5.5	57.5	2.2	7.8	87	19	420
	Max.	67.9	7.9	18.1	111	3.3	21	340	62	
	Min.	0.3	7.4	1.0	22.6	1.7	1.6	13	5.4	
T6	Mean	5.7	8.1	4.7	53.2	2.1	11	65	14	375
	Max.	60.6	9.9	10.1	181	2.8	44	220	29	
	Min.	0.1	7.5	1.2	13.4	1.5	1.7	10	4.3	
CAE	Mean	0.4	7.4	6.2	292	7.1	100	530	130	56,000
	Max.	1.6	7.7	14.5	493	25.3	370	2200	490	
	Min.	0.3	6.9	1.8	10.6	1.4	9.2	51	39	

CAE represents the chlor-alkali effluent and EF_{Hg}^{Sc} is calculated for bottom sediment using normalization with Sc (Hissler and Probst, 2006).

(Syvitski and Morehead, 1999). Mechanical erosion of river basins and fluvial transport of sediment strongly depend on many natural parameters related to topography, soil and rock lithology, climate, hydrology, and land cover. Additionally, anthropogenic influences affect the continental erosion and TSS supply (Walling and Probst, 1997). Thus, deforestation, agricultural and industrial activities increase soil erosion while, at the same time, an important quantity of suspended sediment is trapped by terrestrial reservoirs (Vörösmarty et al., 1997).

The important embankment of the Thur River channel causes negligible riverbank erosion and small variations of the mean annual TSS concentrations between the different sample sites (Table 1). The TSS measured during the study period show lower concentrations than those already observed in the river during the last 30 a, with maximum TSS higher than 100 mg L⁻¹. Temporal variability of daily TSS flux and the low sampling frequency created a lack of representative data at a yearly scale (Coynel et al., 2004). However, the estimation of the weighted average specific flux (based on the Water Agency database) was similar to the values given by Meybeck et al. (2003) for Canadian and French small catchments (20–40 kg km⁻² day⁻¹). The difference observed between the mountainous area (19 kg km⁻² day⁻¹ at T2) and the plain area (10 kg km⁻² day⁻¹ at T6) explains the change in river morphodynamics (slope, elevation). These weak fluxes are representative of the Thur River basin and especially of the important TSS trapping that occurs in the dam reservoir located upstream from T1. Negligible riverbank erosion creates conservative TSS flux all along the Thur channel.

4.3. Chemical evolution of river water

The chemical composition of the Thur river waters evolved between two ends: natural waters,

which directly flow out of the Vosges Mountains (streams) and the CAP effluents. Their chemical evolution depended on the sample station location and was influenced by anthropogenic activities. Natural water was neutral (pH 7.1–7.4) or alkaline with dominant proportions of Ca^{2+} in the total cationic charges and of HCO_3^- in the total anionic load. The CAP effluents were neutral (pH 6.9–7.7) saline water enriched in monovalent cations (70–95% of the total cationic load) and Cl^- (50–80% of the total anionic load).

The DOC increased from upstream to downstream (Table 1). The mean annual concentrations ranged from 1.3 mg L^{-1} at T1 to 2.3 mg L^{-1} at T4. The amount of DOC present in both industrial effluents (CAE and C), up to 25 mg L^{-1}, may affect the increase of organic matter content in the downstream part of the river.

4.4. Total particulate mercury in the river bottom sediment

Results from the river bottom sediment survey for total Hg are illustrated in Fig. 4. For 85 samples collected in December 2001, Hg concentrations in the <2 mm size bottom sediment fraction were measured, while for the other samples (T1–T6), Hg concentrations using both fine (<63 μm) and coarse-silt (63 μm to <2 mm) fractions and the respective abundance of these two size fractions were calculated.

Contamination of sediment with Hg was estimated in the finest fractions (<63 μm) of the bottom sediment, considering first the enrichment (EF_{Hg}^{Sc}) in the mineral fraction (Eq. (3), normalization using Sc – Table 1), and second the enrichment (EF_{Hg}^{OC}) in the organic C fraction (Eq. (4), normalization using OC) as proposed by Hissler and Probst (2006):

$$EF_{Hg}^{Sc} = (Hg/Sc)_{sample}/(Hg/Sc)_{background} \qquad (3)$$
$$EF_{Hg}^{OC} = (Hg/OC)_{sample}/(Hg/OC)_{background} \qquad (4)$$

with $(Hg/Sc)_{background}$ and $(Hg/OC)_{background}$ as the average natural ratios (equalling 1.8×10^{-3} and 2.7×10^{-2}, respectively) measured in the deepest soil horizons of the upper Thur River basin.

4.4.1. Spatial distribution of mercury contamination

The pattern of Hg in sediment followed a distinct pollution plume with an important increase downstream from T3. A high average Hg concentration in the pollution plume (43 μg g^{-1} for the <2 mm particles size) could be found within the first 100 m from the CAP effluent. This maximum was followed by a gradual decline downstream until it reached a constant concentration of approximately 0.4 μg g^{-1} at the confluence with the C channel. Thereafter, an increase in Hg concentration was observed within 5 km (average of 2 μg g^{-1}). Deviation of the river course could also be considered as an indirect source of Hg pollution to the Thur River. The grainsize of the bottom sediment in the
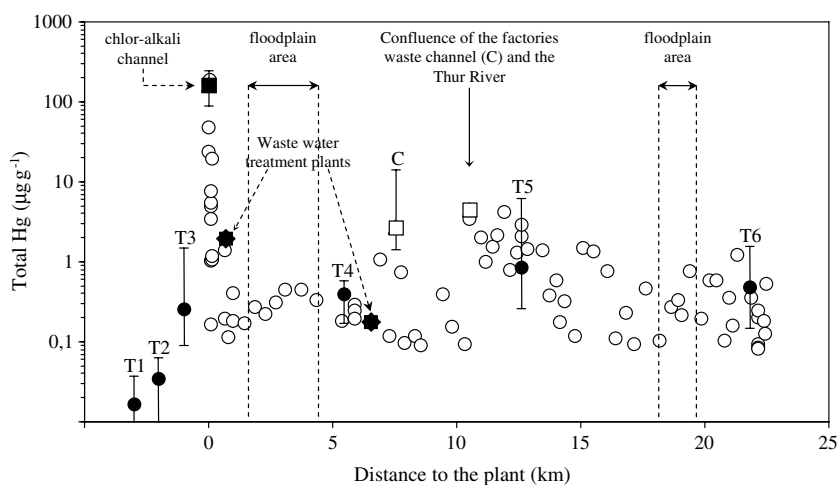

Fig. 4. Spatial distribution of the total mercury concentration in the <2 mm size particles of the Thur River bottom sediments in relation to the distance to the chlor-alkali plant. The black circles and the white square with vertical bars (standard deviation) indicate the median values of mercury concentration calculated for five sampling events (from July 2001 to June 2002), respectively for the different sampling stations (T1–T6) and the industrial channels (C). The other plots represent samples collected downstream from the chlor-alkali effluent in December 2001.

C channel changed in an opposite manner to the one in the river. In this deviation of the main river course, the contribution of fine particles increased during the high flow period, from 0.6% between June and October to 3% between November and March. Thus, high flow produced more particles with higher specific surface area and higher Hg concentration. Consequently, the C channel may have released some Hg enriched sediment into the Thur River during flood events.

4.4.2. Mercury concentration versus size and nature of particles

Bottom sediment grainsize has a strong influence on the distribution of Hg. Trace metals show a strong affinity for fine size particles of stream sediment and their coatings (clay minerals, Fe and Mn oxides, organic matter). The sorption of these elements is more important for the finest particles, which represent the highest specific surface area. Nevertheless, the abundance of Hg in sediment depends on the relative abundance of these size fractions (Probst et al., 1999). In mountainous and embanked rivers, sediment shows a weak maturity with a smaller contribution of clay minerals. The Chemical Index of Alteration (CIA, Nesbitt and Young, 1982) has been shown to be useful to quantify the intensity of weathering in a given basin (Depetris et al., 2003). The CIA values for the Thur River basin ranged from 60 to 65. This represented high-relief areas as well as rivers with high sediment yields. These dynamic conditions mean that Thur

River bottom sediment was depleted in clay minerals (15% of the mineralogical composition) and in fine particles (particles of <63 μm represent 0.1–5% of the bottom sediment) (Fig. 5). Thus, the Thur River bottom sediment principally consisted of silt and fine sand particles of primary minerals (45% quartz and 40% feldspar).

Fine particles (<63 μm) were 5–100 times more concentrated in Hg than the coarse ones (63 μm to 2 mm),where total Hg concentrations ranged from 0.5 to 10 μg g^{-1} and 0.01 to 0.5 μg g^{-1}, respectively (Fig. 5). However, the abundance of the coarse fraction indicated that 80–90% of the total Hg was adsorbed onto silt and sand. Consequently, the coarse fraction could represent the principal reservoir for Hg trapping in the riverbed.

The role of organic matter trapping of Hg in soil and stream sediment of the upper Thur River basin was shown in Hissler and Probst (2006). There, the organic matter has the capacity to control the Hg enrichment due to atmospheric deposition. However, the most polluted part of the river (downstream from T2) indicated important Hg enrichment in both the mineral and organic fractions of the river bottom sediment. No clear relationship was found between Hg concentration and organic C content in the bottom sediment for the downstream stations (Fig. 6, T4–T6) and for the industrial channels (C and CAC), contrary to observations in the upper part of the Thur basin for station T1 and for all the small streams (Hissler and Probst, 2006). Moreover, the Hg enrichment factor
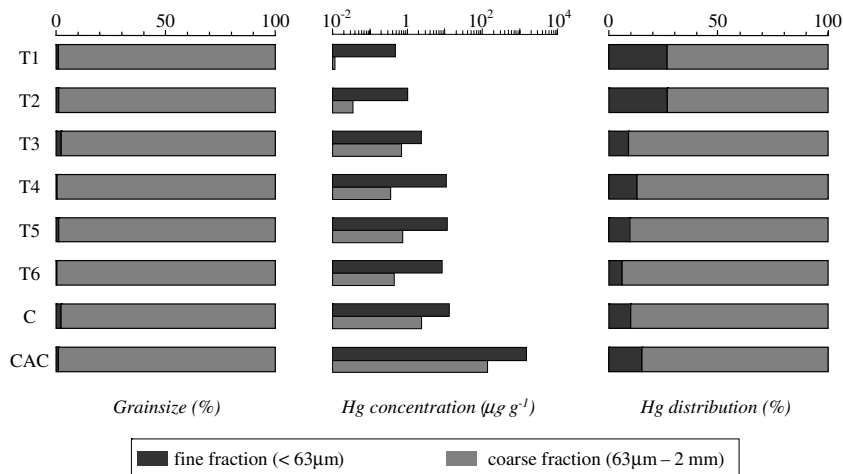

Fig. 5. Percentages of fine and coarse fractions, total mercury concentrations and abundance of mercury in each fraction for the different sampling station of the Thur River basin. CAC represents bottom sediments collected in the chlor-alkali channel.
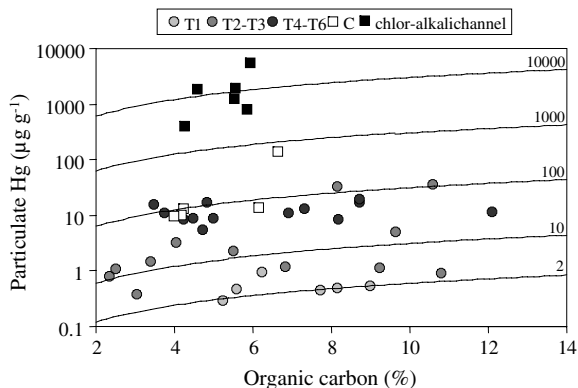
Fig. 6. Relationship between the total Hg concentration and the organic carbon content in the river bottom sediment of the Thur River basin. The lines correspond to Hg enrichment factors from 2 to 10,000 (EF_{Hg}^{OC}), normalized to the organic carbon content (see Hissler and Probst, 2006).

normalized to the organic C content (EF_{Hg}^{OC}, Eq. (4)) largely exceeded 2 for most of the river bottom sediment (except for station T1), indicating that Hg enrichment in bottom sediment was not only due to Hg trapping by organic matter. This result was corroborated by the plot of Hg enrichment factor calculated previously by normalizing to Sc (EF_{Hg}^{Sc}, Eq. (3)) versus the organic C content (Fig. 7): for the upper part of the catchment, the relationship was strong (results from Hissler and Probst, 2006), whereas for the lower part (downstream from the industrial effluents), there was no relationship. Consequently, these results suggest that Hg, in such a
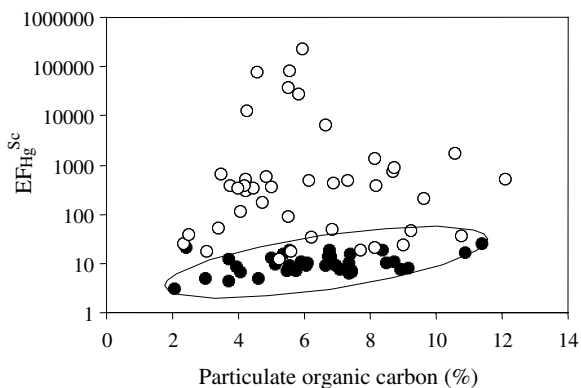
heavily polluted area, is mainly adsorbed onto the mineral fractions of the bottom sediment because the organic matter is rapidly saturated by Hg pollution. Indeed, this hypothesis needs to be confirmed by in situ analyses of Hg of various fractions by geochemical analysis.

4.5. Spatial and seasonal variations of mercury in river water

4.5.1. Total dissolved and particulate mercury in river water

The basin can be divided into two parts according to the location of the confluence between the CAP effluent and the river. Hg_T^d concentrations measured in 2001 and 2002 were relatively constant from T1 to T3 (Table 1). The mean annual Hg_T^d concentrations (0.7–1.3 ng L^{-1}) were similar to that in water found in others fluvial systems (Coquery et al., 1995). Hg_T^p showed higher concentrations than the natural geochemical background (0.03 μg g^{-1}). The diffuse atmospheric pollution due to industrial activity contaminated the grounds of the mountainous region and suspended sediment, which flowed from the river tributaries to the main channel (Hissler and Probst, 2006). However, anthropogenic activities may disturb both of these signals. The highest concentrations measured in July 2001 for the total dissolved Hg at T3 (5.5 ng L^{-1}) and in August 2001 for the TSS Hg concentration (4.9 μg g^{-1}) at T2 illustrated diffuse contamination due to ancient landfill sites and water purification networks. The total dissolved Hg concentrations were higher during the low water period and increased together with the water discharge during the high water period, especially during spring snow melting (Fig. 8). Atmospheric emissions of Hg from the CAP resulted in Hg contamination in the mountainous part of the Thur River basin. Significant quantities of atmospheric Hg may be trapped in the snow during winter and liberated in the stream waters during the spring (Dommergue et al., 2003), increasing the total dissolved Hg concentrations in the mountainous part of this basin.

The impact of the CAP remained the most troublesome for Hg contamination of the aquatic environment. In the alluvial plain area, the industrial Hg input controlled the total Hg concentrations in the water throughout the year. The Hg data collected from T4 to T6 were up to 500 times higher than the upstream concentrations, indicating that Hg pollution from the chlor-alkali effluents was still

Fig. 7. Relationship between organic carbon content and mercury enrichment factors calculated for the mineral fraction of sediment (EF_{Hg}^{Sc} – normalization using Sc). Black circles correspond to stream sediment collected in the upper Thur River basin (Hissler and Probst, 2006) and open circles were obtained in this study.
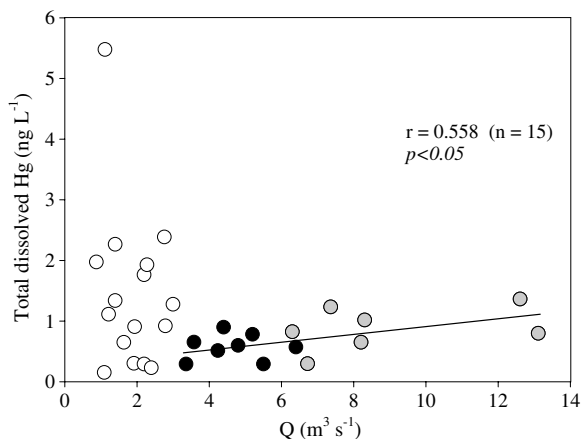
Fig. 8. Relationship between total dissolved mercury and water discharge upstream from the confluence between the chlor-alkali effluents and the Thur River. Open circles correspond to low water period (June to October), black circles to high level water of winter (November to January), and grey circles to high level water of spring, i.e., snow melting periods (February to May).
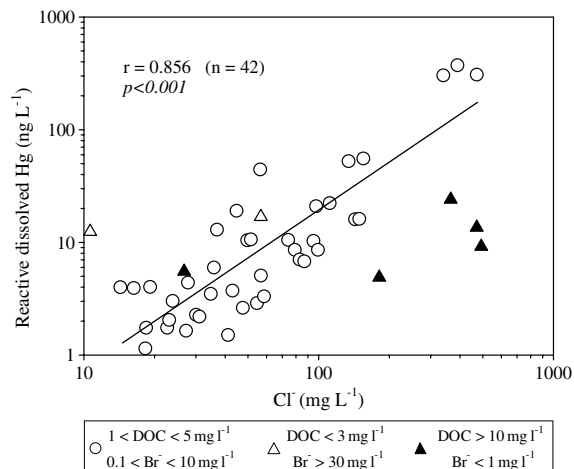

Fig. 9. Relationship between chloride and dissolved reactive mercury in the Thur River downstream from the chlor-alkali plant. The line defines the trend of this relation. The triangles illustrate the influence of bromide and DOC concentrations on the reactive dissolved mercury concentration.

important in spite of the drastic Hg reductions that the CAP initiated in 1970. The total Hg concentrations (dissolved + particulate) measured in the effluents often exceeded the international drinking water standard (1000 ng L^{-1}, EEC, 1980), resulting in significant Hg pollution of river water, as seen in June 2002 at T4 (1300 ng L^{-1}). In general, after the confluence with the river, the Hg polluted effluents were progressively diluted by the input of additional water (Table 1). Nevertheless, high concentrations of Hg in water at the outlet of the basin; were found at T6 as 65 ng L^{-1} in solution and 13.9 µg g^{-1} in the particulate fraction.

4.5.2. Reactive dissolved mercury in river water

Hg_R^d was only measured for the most polluted sites (Table 1; CAE, C, T4, T5, T6). The Hg_R^d contribution to the total dissolved Hg varied more in the chlor-alkali channel (from 2% in March to 86% in September), where the discharge and temperature variations were more significant than in the Thur River between both hydrological periods. In the main river channel, the contribution of Hg_R^d ranged from 5% to 25% in the high water periods and from 2% to 40% in the low water periods. During low water flow, it seemed that Hg_R^d corresponded to Hg mainly complexed with Cl when the DOC concentration was <5 mg L^{-1} (Hissler et al., in press). There was a good relationship between Hg_R^d and Cl concentration downstream from the CAP ($R^2 = 0.74$, Fig. 9).

4.6. Mercury transport and partitioning in the Thur River system

Variations of Hg and its distribution between aqueous and particulate phases are controlled by natural processes (erosion, weathering, atmospheric deposition), anthropogenic input, and the exchange of Hg between different compartments of an aquatic system. The hydrological conditions and the distance between samples collected from the chlor-alkali effluents were two of the most important parameters that control the total Hg partitioning in the water column of the Thur River: (a) the hydrological conditions mainly controlled the TSS concentration, which is one of the most important factors controlling particulate Hg (Quesmerais et al., 1998), and (b) when the distance between the chlor-alkali effluent input and the sample site increases, the possibility of exchange between the dissolved and the particulate phases increases and is controlled by changes in the physico-chemical conditions of the river water.

4.6.1. Mercury partitioning between dissolved and particulate phases

The behaviour of Hg in aquatic systems depends on its distribution between their dissolved and particulate forms. For example, the transport of Hg through aquifers is strongly influenced by partitioning between solids and solution. To understand this process and to be able to predict it quantitatively,

the calculation of the K_d coefficient (ratio between the Hg concentration in the particulate ($\mu g\,g^{-1}$) and dissolved phase ($ng\,L^{-1}$)) is widely used (Benoit, 1995; Gaiero et al., 2003).

Major factors that control the K_d variations (Fig. 10) are the total suspended matter (TSS), water pH, DOC, and inorganic (Cl) ligands (Dzombak and Morel, 1990; Gaiero et al., 2003; Ravichandran, 2004). Contrary to that observed generally, K_d decreased when TSS increased particularly in the upper part of the basin (Fig. 10a). The K_d was controlled by the dissolved Hg (not by the TSS), which increases in the upper basin (Fig. 8) due to the release of Hg during snow melting (Dommergue et al., 2003).

The pH (Fig. 10b) controls most of the processes that affect the partitioning of trace elements between particulate and dissolved fractions. Generally, an increase of pH leads not only to cation adsorption, but also to anion desorption that increases the quantity of inorganic and organic ligands in solution (Dzombak and Morel, 1990). The combination of both of these processes affected Hg desorption for

water pH higher than 7.5. The K_d decreased in Thur River water, particularly during low flow, when the pH increased due to the increase of dissolved Hg complexation by organic and inorganic ligands (Fig. 10b). The relative importance of each ligand depended on the concentrations of both the metal and the ligand and the binding strength of the metal–ligand complex. Without organic ligands, $Hg(OH)_2$ and $HgCl_2$ are the two dominant Hg species in natural water (Dyrssen and Wedborg, 1991). When the Cl concentration increased (Fig. 10c), hydroxyl complexes, which dominated in low Cl solutions, were replaced by chlorocomplexes (Morel, 1983), decreasing Hg adsorption on aqueous particulates (Forbes et al., 1974; Randle and Hartmann, 1987). However, Cl and hydroxide are unlikely to compete with organic matter for binding in most freshwater systems. The stability constants for Hg–DOC complexes reported in the literature are about 10^{20}–10^{28} in aquatic systems (Benoit et al., 2001; Haitzer et al., 2002; Lamborg et al., 2003) and higher than 10^{30} in the wastewater of treatment plants (Hsu and Sedlack, 2003). These
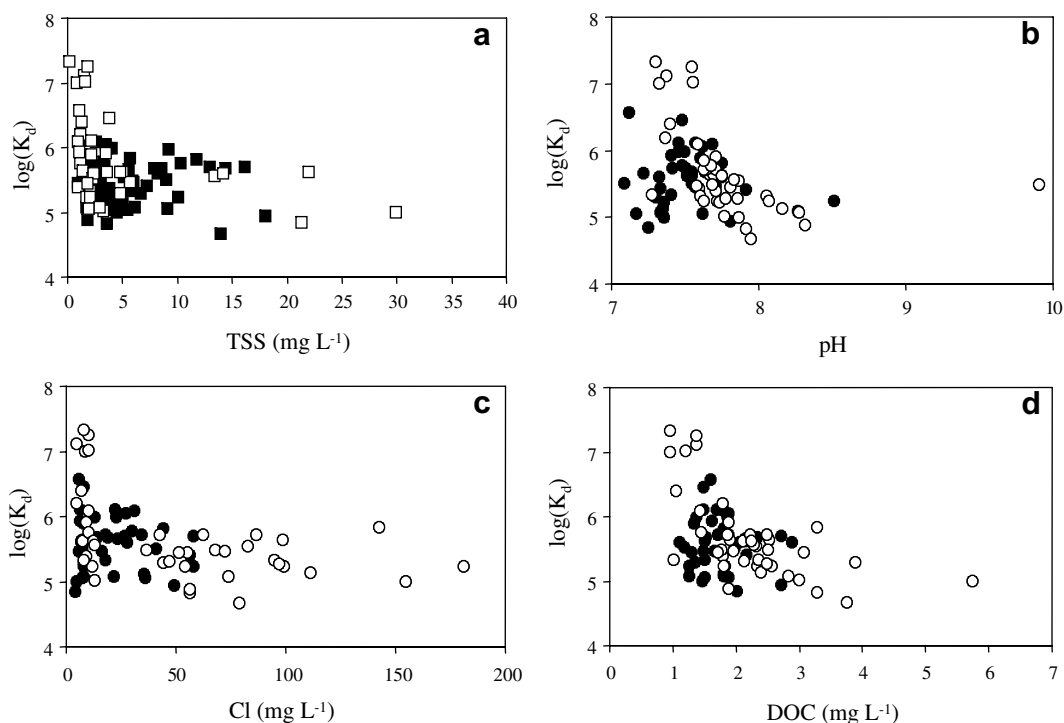

Fig. 10. Relationships between Hg partitioning coefficient ($\log K_d$ between particulate ($\mu g\,g^{-1}$) and dissolved ($ng\,L^{-1}$) Hg) and (a) total suspended sediment concentration (TSS), (b) pH, (c) chloride concentration and (d) dissolved organic carbon (DOC) concentration in the water from the Thur River. Open squares represent the samples collected upstream from the chlor-alkali plant and black squares the samples collected downstream from the plant. Open circles correspond to low level water and black circles to high level water.

stability constants are much larger than the ones reported for Hg–Cl complexes (10^7–10^{14}) or Hg–OH complexes (10^{10}–10^{22}). Moreover, at pH higher than 7, DOC is more negatively charged, and therefore, more likely to complex (Barkay et al., 1997). Depending on the anthropogenic input into the Thur River from April to September, DOC would constitute the main ligand for Hg complexation (Driscoll et al., 1995), as was observed for DOC concentrations higher than 1.5 mg L^{-1} (Fig. 10d).

Consequently, the longitudinal profiles of the evolution of K_d between T1 and T6 were quite different during the two hydrological periods (Fig. 11). During the low water flow (September 2001), K_d progressively decreased from upstream to downstream, whereas during high flow in the spring (March 2002), K_d remained constant in the upper part of the Thur River from T1 to T4 and increased in the lower part from T4 to T6. At station T4, K_d was comparable during both periods and close to that of site CAE ($\log K_d = 5.5$), demonstrating that at T4, the distribution of Hg between the two phases was greatly influenced by the effluent. During the spring high flow, the lower K_d was controlled in the upper part of the Thur River by the increase of dissolved Hg due to the release of Hg during snow melting (Dommergue et al., 2003). In contrast in the lower part of the Thur River, the increase of K_d during the high water flow could be attributed to remobilization of particulate Hg from river bed sediment (1500 t of sediment was remobilized between T4 and T5, Hissler, 2003). During the low flow, the K_d decrease in the upper part of the Thur River is attributed to the 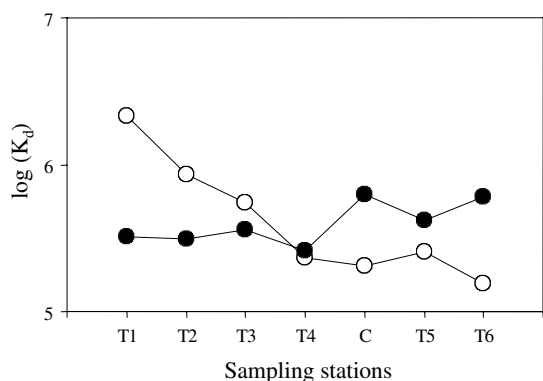increase of dissolved Hg due to Hg complexation by dissolved organic (Fig. 10d) and inorganic (Fig. 10c) ligands, which increased from T1 to T3 (Table 1). Finally, during low flow, the K_d was controlled from T4 to T5 by the chlor-alkali effluents. Between T5 and T6, the K_d decrease could be attributed both to sedimentation processes (1800 t of sediment deposited between T5 and T6, Hissler, 2003), which decreased the particulate Hg, and to methylation processes (Remy, 2002; Remy et al., 2002, 2003a), which increased the dissolved Hg in the water column.

4.6.2. Seasonal mercury transport between dissolved and particulate phases

The concentration of Hg in the dissolved and particulate phases and river discharge at different gauging stations allowed calculation of the amount of Hg transported in solution and in suspension. The spatial evolution of dissolved and particulate total Hg flux was determined for the upstream to downstream parts of the Thur River basin (Fig. 12). Gains or losses of Hg between two sample stations were also estimated (Fig. 12) following the procedure of Meade et al. (1985). For each river section, the annual input–output balance of particulate Hg flux allowed calculation of the amount of Hg lost (input − output < 0) or gained (input − output > 0) from one station to another. The corresponding average Hg concentration in the flux of sediment deposited or remobilized in this section of the Thur River was calculated and compared with the median concentration of Hg found in bottom sediment. Comparison of the calculated Hg flux and measured Hg concentrations validates the input–output budget calculation for Hg transport (Fig. 13). The most important deviation (section T3–T4) between these two values came from the extreme Hg concentrations measured in the chlor-alkali channel that was not representative of the major part of the T3–T4 section of the Thur River.

At station T3, Hg flux was negligible compared to the annual quantity of Hg released in the river system by the chlor-alkali plant. Consequently, the specific annual Hg flux increased from 5 μg m^{-2} a^{-1} at T3 to 260 μg m^{-2} a^{-1} at T4.

Between July 2001 and June 2002, Hg was principally transported by suspended particles (65–84%, respectively, during low and high flow), but the aqueous phase was not a negligible vector for Hg transportation inside the Thur River basin. This result was similar to Probst et al. (1999), who esti-

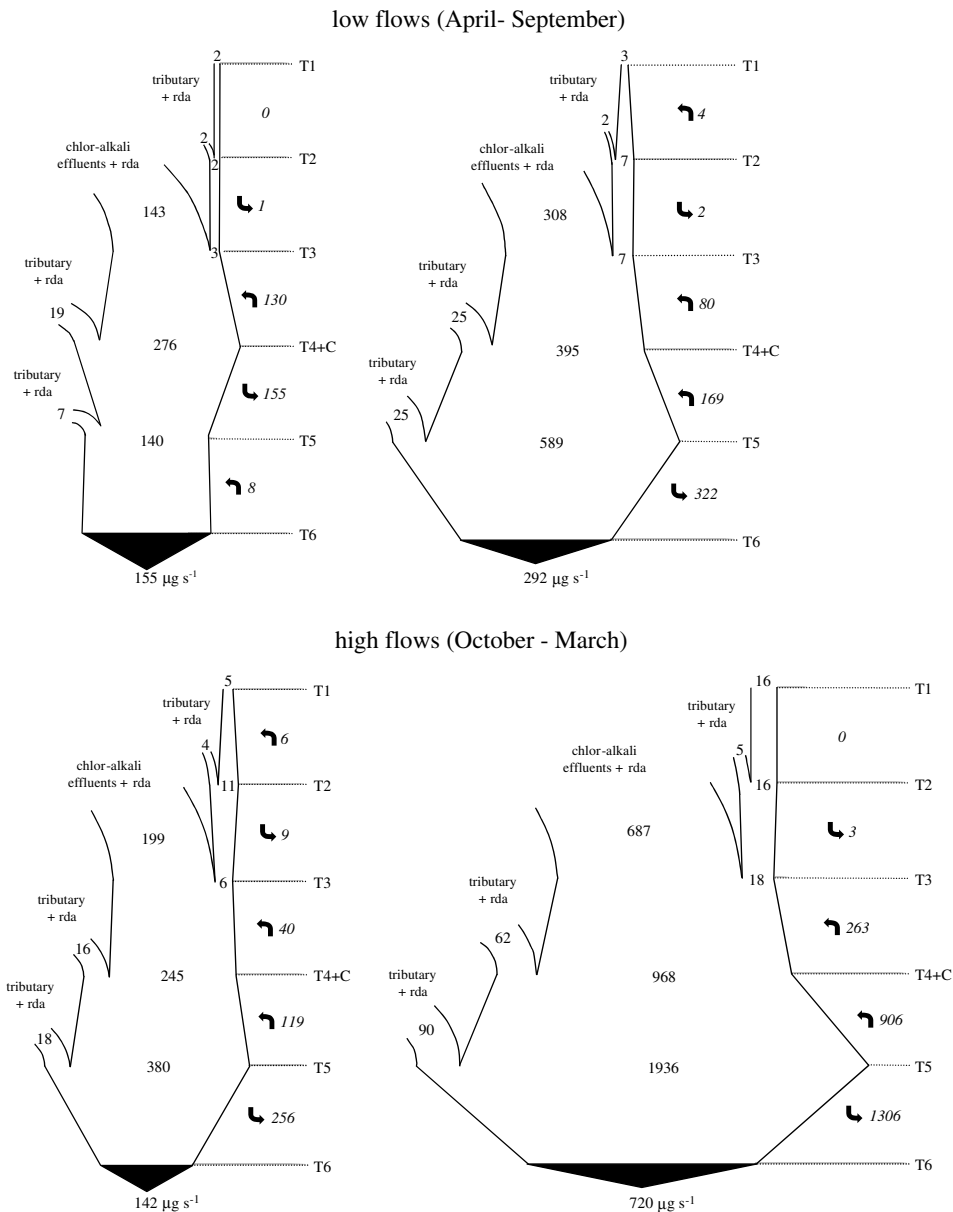Fig. 11. Spatial and seasonal evolution of Hg distribution coefficient ($\log K_d$) between particulate (μg g^{-1}) and dissolved (ng L^{-1}) phases. Open circles correspond to low flow of September 2001 and black circles to high flow of March 2002.

low flows (April- September)

high flows (October - March)

Fig. 12. Spatial evolution of mercury fluxes ($\mu g \, s^{-1}$) in dissolved (left side) and particulate (right side) phases in the Thur River basin during high and low water periods. *rda* represent the residual drainage basin, up and down black arrows situated on the right side of each diagram represent respectively gains and losses of mercury between two sampling stations.

mated the particulate Hg flux at 1166 $\mu g \, s^{-1}$ during the high flow of February 1996, i.e., 81% of the total Hg (dissolved + particulate) exported outside the Thur River basin.

The particulate flux of Hg appeared to be higher during the high water period (84 $\mu g \, m^{-2} \, a^{-1}$ at T6) than during low flow (34 $\mu g \, m^{-2} \, a^{-1}$ at T6). This may be due to higher industrial input, higher suspended river sediment transport, and more remobi-

lization of river bottom sediment. The bottom sediment remobilization was the most important process that controls the gain of particulate Hg between T3 and T5. This river section was totally embanked and may present a higher rate of riverbed erosion than for the other sections. From T5 to T6, the important loss (60%) of particulate Hg may be attributed to sedimentation processes that appeared in the small flood plain areas of the basin.
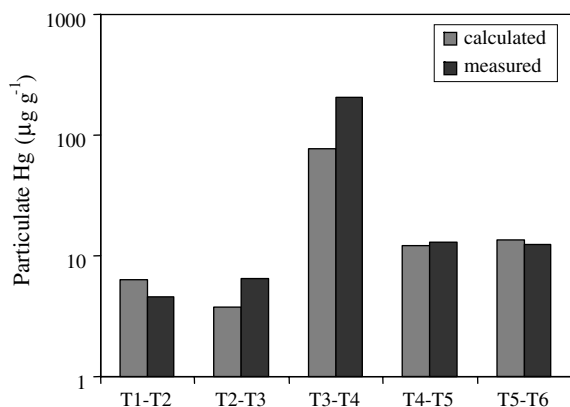
Fig. 13. Comparison between Hg concentration measured in sediment of eight sample stations and Hg concentration estimated using flux calculations.

On the other hand, the quantities of dissolved Hg transported during both hydrological periods were similar, with a specific transport rate of approximately 18 $\mu g \, m^{-2} \, a^{-1}$ at T6. Nevertheless, the different hydrologic conditions that existed during both periods created some differences in the dissolved Hg mass balance between the different stations. During the high water period, assuming that the ratio between dissolved and particulate flux of Hg did not differ from the chlor-alkali effluent to the outlet of the basin (average ratio of 0.24 with 19% variation), the authors consider the exchanges between the particles and the solution negligible for the whole river channel of the plain area. The situation was quite different during low flow, where the same ratio (dissolved versus particulate) for the high flow (0.24) was applied to the particulate Hg gains or losses during the low water period between two stations. Then, a theoretical value for dissolved Hg gains or losses was estimated and compared to the first calculation (input–output balance). The difference between the two values (input–output value minus theoretical ratio value) allowed assessment of the flux of dissolved Hg adsorbed (difference < 0) or desorbed (difference > 0) from particles. From T3 to T4, about 85% of the dissolved Hg gains may be explained by desorption from suspended sediment. Between T5 and T6, this latter process was not sufficient to explain the important gains of total dissolved Hg. The desorption of Hg from the bottom sediment trapped in the small flood plain areas of this section of the Thur River may contribute about 10% of the dissolved Hg released to the water column. The loss of Hg that appeared during low flow

from T4 to T5 may be attributed to river water infiltration to groundwater in this section of the river (Duprat et al., 1979; Esteves, 1989). Conversely, such Hg losses may be due to methylation processes (Remy et al., 2003a) that lead to efficient Hg absorption by organisms or demethylation processes releasing Hg to the atmosphere (Winfrey and Rudd, 1990; Gilmour and Henry, 1991).

4.7. Impact of anthropogenic activities on the annual budget of mercury

The mountainous area that represents 60% of the Thur River basin and the plain area located downstream of the chlor-alkali plant play an opposite role in the annual cycle of Hg (Fig. 14). Historical and current Hg atmospheric emissions (100 kg a^{-1}) from the CAP are mostly responsible for Hg contamination of soil and streambed sediment in the upper Thur River basin. An important part of the atmospheric Hg deposited on this mountainous area is fixed by the organic matter and migrates through the soil profile, producing high Hg enrichment (Hissler and Probst, 2006). They both create complexes with high stability, indicating that soil makes up the first large reservoir for local anthropogenic Hg trapping (19,000 kg, i.e., 90 mg m^{-2}) and that Hg is stored for a long period of time in soil (>10^5 a). Soil erosion in the upper basin released a negligible quantity of Hg to streams (0.1 kg a^{-1}, i.e., <1 $\mu g \, m^{-2} \, a^{-1}$) in comparison to the anthropogenic effluents (19 kg a^{-1}, i.e., 70 $\mu g \, m^{-2} \, a^{-1}$).

The dynamics of Hg are completely different in the plain area, due to the anthropogenic influences on the riverbed (water pollution, river embankment). Some of these changes, which occurred during the 1980s, made the river more dynamic and caused more erosion of riverbed sediment, but negligible riverbank erosion. In these conditions, bottom sediment is coarse (Fig. 4) and not sufficient to trap a significant quantity of Hg, causing a small accumulation of Hg in the top 10 cm of the river bottom sediment from T3 to the outlet of the basin (2 kg, i.e., 4 mg m^{-2}). Consequently, the annual export of Hg through the Thur River corresponded to the input of Hg from anthropogenic activities (19 kg a^{-1}, i.e., 70 $\mu g \, m^{-2} \, a^{-1}$) and the annual budget of Hg transportation in the Thur River water was conservative in the plain area, involving a short residence time for Hg (1 month). Climatic and hydrologic conditions that dominated during the summer involved a desorption Hg flux from sus-
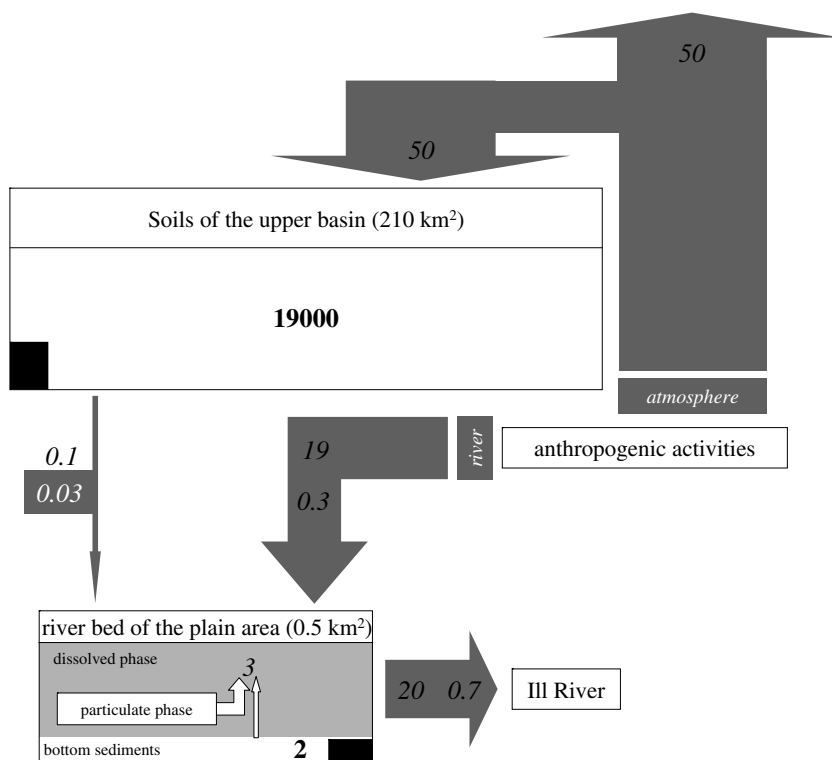
Fig. 14. Annual budget of total mercury in the Thur River basin. Numbers in bold correspond to the stocks (kg) and numbers in italics correspond to the fluxes (kg y^{-1}). The results for the upper basin are from Hissler and Probst (2006). We present the methylmercury contribution (white police), according to the results of Remy et al. (2003a).

pended (2.0 kg a^{-1}) and bottom (0.1 kg a^{-1}) sediment to the river water that represented 3 kg a^{-1}, i.e., 11 µg m^{-2} a^{-1}. This represents 15% of the total Hg export outside the watershed (20 kg a^{-1}) and could greatly contribute to the Hg transfer from the river water to groundwater in this area, where direction of the water exchanges is from the river to the groundwater (Duprat et al., 1979; Esteves, 1989).

As a result of the high level of toxicity of MeHg, it seemed important to evaluate its contribution to the total Hg mass balance. Using the results obtained by Remy et al. (2002, 2003a) for the MeHg amount in suspended and bottom sediment and soil of the Thur River basin, the annual MeHg budget was also estimated (Fig. 14). The estimated average methylation rates ranged from 1% of the total Hg in the river bottom sediment to 3.5% in the suspended sediment downstream to T4 (Remy et al., 2002, 2003a). The flux of Hg obtained (0.1–2.6 µg m^{-2} a^{-1}) is similar to that found in other European and North American river catchments, ranging from 0.1 to 5.9 µg m^{-2} a^{-1} (Johansson et al., 1991; Lee et al., 1995; St. Louis et al., 1996). It was shown that from the input of anthropogenic Hg to the outlet of the basin, the MeHg flux ranged from 1.5% to 4% of the total Hg flux. Thus, the hydrologic and climatic conditions may be favourable for Hg methylation in the downstream part of the Thur River. Conversion to MeHg could decrease the quantity of Hg adsorbed on bottom sediment and favor the volatilization of Hg into the atmosphere or its absorption by aquatic organisms. The concentration of MeHg measured in benthic organisms corresponds to 20% of the total Hg (average concentration of 350 ± 105 ng g^{-1} – Remy, 2002; Remy et al., 2002) indicating the potential for bioaccumulation of Hg (Tremblay, 1999).

5. Conclusions

The dynamic nature of Hg was studied during one climatic cycle in the Thur River watershed, which is heavily polluted by anthropogenic activities, principally by a CAP. In spite of decreases in the release of industrial Hg to the Thur River during

the last 30 a, the investigation showed persistent Hg contamination of different compartments of the river. Concentrations of Hg measured for Thur River sediment and water downstream from the CAP were up to 500 times higher than Hg concentrations measured upstream.

Variations of Hg and its dynamics were controlled by hydroclimatic conditions, river morphology, river water chemistry, and anthropogenic inputs. Upstream from the CAP, Hg partitioning was principally controlled by snow melting during spring high flow, while during low flow, Hg was primarily adsorbed onto the particulates. Downstream from the CAP, the water chemistry induced Hg partitioning in the water column. During high water levels, Hg showed a higher affinity for particulate phases as indicated by TSS concentration increases and dilution of ligand concentrations. Particulate Hg flux was five times higher than that for dissolved Hg. Conversely, the exchange between the particulate Hg and dissolved Hg were negligible in the river channel from the input of the industrial effluent to the watershed outlet. The hydrological conditions present during the low water period greatly increased the transformation of Hg in the water column. For pH higher than 7.5, Hg was easily desorbed from the suspended particles, forming inorganic (chloride, hydroxyl) or DOC dissolved complexes. Moreover, during this latter period, reactive dissolved Hg corresponded with Hg mainly complexed with Cl for the lowest DOC concentrations.

In the most polluted part of the river, the bottom sediment samples showed important Hg enrichments in comparison to the organic C content, indicating that the organic fraction of sediment may complex a small quantity of the Hg released in the aquatic environment. Consequently, these results suggest the possibility for Hg, in such a heavily polluted area, to be mainly adsorbed onto the mineral fractions of bottom sediment because the initial input of the Hg is rapidly absorbed by the organic matter portion of the bottom sediment. This caused a small portion of Hg to be stored in the top 10 cm of the bottom sediment from the CAP to the outlet of the basin. Therefore, the annual export of Hg through the Thur River is approximately equal to the input of Hg from anthropogenic activities. The annual budget of Hg transport in the Thur River appears to be conservative in the plain area, involving a short residence time – about 1 month – of the Hg pollution in the river channel.

References

Bakir, F., Damluji, S.F., Amin-Zaki, L., Murthada, M., Khalidi, A., Al-Rawi, N.Y., Tikriti, S., Dhahir, H.I., Clarkson, T.W., Smith, J.C., Doherty, R.A., 1973. Methylmercury poisoning in Iraq. Science 181, 230–241.

Barkay, T., Gillman, M., Turner, R.R., 1997. Effects of dissolved organic carbon and salinity on bioavailability of mercury. Appl. Environ. Microbiol. 63, 4267–4271.

Benoit, G., 1995. Evidence of the particle concentration effect for lead and other metals in fresh waters based on clean technique analyses. Geochim. Cosmochim. Acta 59, 2677–2687.

Benoit, J.M., Mason, R.P., Gilmour, C.C., Aiken, G.R., 2001. Constants of mercury binding by dissolved organic matter isolated from the Florida Everglades. Geochim. Cosmochim. Acta 65, 4445–4451.

Biester, H., Muller, G., Schöler, H.F., 2002a. Estimating distribution and retention of mercury in three different soils contaminated by emissions from chlor-alkali plants: Part I. Sci. Total Environ. 284, 177–189.

Biester, H., Muller, G., Schöler, H.F., 2002b. Binding and mobility of mercury in soils contaminated by emissions from chlor-alkali plants. Sci. Total Environ. 284, 191–203.

Birkett, J.W., Noreng, J.M.K., Lester, J.N., 2002. Spatial distribution of mercury in the sediments and riparian environment of the River Yare, Norfolk, UK. Environ. Pollut. 116, 65–74.

Calasans, C.F., Malm, O., 1997. Elemental mercury contamination survey in a chlor-alkali plant by the use of transplanted Spanish moss Tillandsia usneoides. Sci. Total Environ. 208, 165–177.

Coquery, M., Cossa, D., Martin, J.M., 1995. The distribution of dissolved and particulate mercury on three Siberian estuaries. Water Air Soil Pollut. 80, 653–664.

Coquery, M., Cossa, D., Sanjuan, J., 1997. Speciation and sorption of mercury in two macro-tidal estuaries. Mar. Chem. 58, 213–227.

Coynel, A., Schäfer, J., Hurtrez, J.-E., Dumas, J., Etcheber, H., Blanc, G., 2004. Sampling frequency and accuracy of SPM flux estimates in two contrasted drainage basins. Sci. Total Environ. 330, 233–247.

Depetris, P.J., Probst, J.-L., Pasquini, I.P., Gaiero, D., 2003. The geochemical characteristics of the Parana River suspended sediment load. An initial assessment. Hydrol. Proc. 17, 1267–1277.

Dommergue, A., Ferrari, C., Gauchard, P.-A., Boutron, C.F., Poissant, L., Pilote, M., Jitaru, P., Adams, F.C., 2003. The

fate of mercury species in a sub-arctic snowpack during snowmelt. Geophys. Res. Lett. 30, 1621.

Driscoll, C.T., Blette, V., Yan, C., Schofield, C.L., Munson, R., Holsapple, J., 1995. The role of dissolved organic carbon in the chemistry and bioavailability of Hg in remote Adirondack. Water Air Soil Pollut. 80, 499–508.

Duprat, A., Simler, L., Valentin, J., 1979. The phreatic groundwater of the Rhine plain in Alsace. Sciences Géologiques Mémoires 60, University of Strasbourg, France (in French).

Dyrssen, D., Wedborg, M., 1991. The sulfur–mercury (II) system in natural waters. Water Air Soil Pollut. 56, 507–519.

Dzombak, D.A., Morel, F.M.M., 1990. Surface Complexation Modelling. Hydrous Ferric Oxide. John Wiley and Sons, New York.

EEC (European Economic Community), 1980. Council Directive 80/778/EEC of 15 July 1980 relating to the quality of water intended for human consumption. Official Journal L 229, pp. 11–29 (in French).

Esteves, M., 1989. Study and modeling of the relations between groundwater and river in the Ried of Colmar (Haut-Rhin, France). Ph.D. Dissertation, University Louis Pasteur, Strasbourg (in French).

Ferrara, R., Maserti, B.E., Edner, H., Ragnarson, P., Svanberg, S., Wallinder, E., 1992. Mercury emissions into the atmosphere from a chlor-alkali complex measured with the LIDAR technique. Atmos. Environ. 26A, 1253–1258.

Forbes, E., Posner, A.M., Quirk, J.P., 1974. The specific adsorption of inorganic Hg(II) species and Co(III) complex ions on goethite. J. Coll. Int. Sci. 49, 403–409.

Gaiero, D.M., Probst, J.-L., Depetris, P.J., Bidart, S.M., Leleyter, L., 2003. Iron and other transition metals in Patagonian riverborne and windborne materials: geochemical control and transport to the southern South Atlantic Ocean. Geochim. Cosmochim. Acta 67, 3603–3623.

Gilmour, C.C., Henry, E.A., 1991. Mercury methylation in the aquatic systems affected by acid deposition. Environ. Pollut. 71, 131–169.

Haitzer, M., Aiken, G.R., Ryan, J.N., 2002. Binding of mercury(II) to dissolved organic matter: the role of mercury-to-DOM concentration ratio. Environ. Sci. Technol. 36, 3564–3570.

Hissler, C., 2003. Dynamic and budget of dissolved and particulate mercury in polluted hydrosystems. Application of the Thur River catchment (Vosges Mountains, France). Ph.D. Dissertation, University Louis Pasteur, Strasbourg, France (in French).

Hissler, C., Probst, J.-L., 2006. Impact of mercury atmospheric deposition on soils and streams in a mountainous catchment (Vosges, France) polluted by chlor-alkali industrial activity: the important role of the organic matter. Sci. Total Environ. 361, 163–178.

Hissler, C., Remy, S., Probst, J.-L., 2003. Natural and anthropogenic contributions to mercury in soils and stream sediments of the upper Thur River basin (Alsace, France). J. Phys. IV France 107, 621–624.

Hissler, C., Probst, J.-L., Mortatti, J., in press. Annual inorganic mercury speciation in river water disturbed by chlor-alkali effluents: role and competition of ligands (Cl^-, Br^-, DOC). Geochim. Brasiliensis.

Hsu, H., Sedlack, D.L., 2003. Strong Hg(II) complexation in municipal wastewater effluent and surface waters. Environ. Sci. Technol. 37, 2743–2749.

Johansson, K., Aastrup, M., Andersson, A., Bringmark, L., Iverfeldt, A., 1991. Mercury in Swedish forest soils and waters: assessment of critical load. Water Air Soil Pollut. 56, 267–281.

Lamborg, C.H., Tseng, C.M., Fitzgerald, W., Balcom, P.H., Hammerschmidt, C.R., 2003. Determination of the mercury complexation characteristics of dissolved organic matter in natural waters with "reducible mercury" titrations. Environ. Sci. Technol. 37, 3316–3322.

Lee, Y.H., Bishop, K., Petterson, C., Iverfeldt, A., Allard, B., 1995. Subcatchment output of mercury and methylmercury at Svartberget in Northern Sweden. Water Air Soil Pollut. 80, 455–465.

Lodenius, M., 1998. Dry and wet deposition of mercury near a chlor-alkali plant. Sci. Total Environ. 213, 53–56.

Maserti, B.E., Ferrara, R., 1991. Mercury in plants, soil and atmosphere near a chlor-alkali complex. Water Air Soil Pollut. 56, 15–20.

Mason, R.P., Fitzgerald, W.F., Hurley, J.P., Hanson, A.K., Donaghay, P.L., Sieburth, J.M., 1993. Mercury biogeochemical cycling in a stratified estuary. Limnol. Oceanog. 38, 1227–1241.

Meade, R.H., Dunne, T., Ritchey, J.E., Santos, U.M., Salati, E., 1985. Storage and remobilization of suspended sediment in the lower Amazon River of Brazil. Science 228, 488–490.

Menendez-Navarro, A., 1996. A world without sun. The health of workers of the Alamaden mine: 1750–1900. Chronica Nova Collection of Historical Studies no. 43, University de Castilla-La Mancha, Granada (in Spanish).

Meybeck, M., Laroche, L., Dürr, H.H., Syvitski, J.P.M., 2003. Global variability of daily total suspended solids and their fluxes in rivers. Global Planet. Change 39, 65–93.

Morel, F.M.M., 1983. Principles of Aquatic Chemistry. John Wiley and Sons, New York.

Nesbitt, H.W., Young, G.M., 1982. Early Proterozoic climates and plate motions inferred from major element chemistry of lutites. Nature 299, 715–717.

Nriagu, J.O., Pacyna, J.M., 1988. Quantitative assessment of worldwide contamination of air, water and soils by trace metals. Nature 333, 134–139.

Osame, M., Takizawa, Y., 2001. Methylmercury Poisoning in Minamata and Niigata, Japan. Japan Public Health Association, Tokyo.

Probst, J.-L., Messaitfa, A., Krempp, G., Behra, P., 1999. Fluvial transports of mercury pollution in the Ill river basin (North-Eastern France): partitioning into aqueous phases, suspended matters and bottom sediments. In: Ebinghaus, R., Turner, R.R., de Lacerda, L.D., Vasiliev, O., Salomons, W. (Eds.), Mercury Contaminated Sites: Characterization, Risk Assessment and Remediation. Springer-Verlag, Berlin, Heidelberg, pp. 501–520.

Quesmerais, B., Cossa, D., 1997. Procedures for sampling and analysis of mercury in natural waters. Rapport Scientifique et Technique Centre St. Laurent, Canada.

Quesmerais, B., Cossa, D., Rondeau, B., Pham, T.T., Fortin, B., 1998. Mercury distribution in relation to iron and manganese in the St. Lawrence River. Sci. Total Environ. 213, 193–201.

Randle, K., Hartmann, E.H., 1987. Application of the continuous flow stirred cell (CSFC) technique to adsorption of zinc, cadmium and mercury on humic acids. Geoderma 40, 281–296.

Ravichandran, M., 2004. Interactions between mercury and dissolved organic matter – a review. Chemosphere 55, 319–331.

Remy, S., 2002. Mercury speciation in soils and river waters. Application of the Thur River catchment (Alsace, France). Ph.D. Dissertation, University Louis Pasteur, Strasbourg, France (in French).

Remy, S., Probst, J.-L., Prudent, P., Krempp, G., 2002. Mercury contents and speciation in soils and river waters of an industrialised catchment, the Thur river basin (Alsace). Contribution of the atmospheric deposition. Pollut. Atmos. 173, 123–135.

Remy, S., Prudent, P., Hissler, C., Probst, J.-L., 2003a. Mercury speciation in soils and river sediments of the Thur river basin (Alsace, France). J. Phys. IV France 107, 1131–1134.

Remy, S., Prudent, P., Hissler, C., Probst, J.-L., Krempp, G., 2003b. Total mercury concentration in an industrialized catchment, the Thur river basin (Northeastern France): geochemical background level and contamination factor. Chemosphere 52, 635–644.

Schuster, E., 1991. The behaviour of mercury in the soil with special emphasis on complexation and adsorption processes, a review of the literature. Water Air Soil Pollut. 56, 667–680.

Sensen, M., Richardson, D.H.S., 2002. Mercury levels in lichens from different host trees around a chlor-alkali plant in New Brunswick, Canada. Sci. Total Environ. 293, 31–45.

St. Louis, V.L., Rudd, J.W.M., Kelly, C.A., Beaty, K.G., Flett, R.J., Roulet, N.T., 1996. Production and loss of methylmercury and loss of total mercury from boreal forest catchments containing different types of wetlands. Environ. Sci. Technol. 30, 2719–2729.

Syvitski, J.P.M., Morehead, M., 1999. Estimating river-sediment discharge to the ocean: application to the Eel margin, Northern California. Mar. Geol. 154, 13–28.

Tremblay, A., 1999. Bioaccumulation of mercury and methylmercury in invertebrates from natural boreal lakes. In: Lucotte, M., Schetagne, R., Thérien, N., Langlois, C., Tremblay, A. (Eds.), Mercury in the Biogeochemichal Cycle. Springer, Berlin, pp. 89–113.

Vernet, J.P., Thomas, R.L., 1972. Mercury in the environment and the role of sedimentary geology. Bull. Mining Geol. Res. Bureau (BRGM), section III, pp. 43–61 (in French).

Vörösmarty, C., Meybeck, M., Fekete, B., Sharma, K., 1997. The potential impact of neo-castorization on sediment transport by the global network rivers. In: Walling, D.E., Probst, J.-L. (Eds.), Human impact on erosion and sedimentation. IAHS Publication, no. 245, pp. 261–273.

Walling, D.E., Probst, J.-L. (Eds.), 1997. Human Impact on Erosion and Sedimentation. International Association of Hydrological Processes, Publication No. 245. IAHS Press.

Winfrey, M.R., Rudd, J.W.M., 1990. Environmental factors affecting the formation of methylmercury in the low pH lakes. Environ. Toxicol. Chem. 9, 853–865.